Distribution Agreement

In presenting this thesis as a partial fulfillment of the requirements for a degree from Emory University, I hereby grant to Emory University and its agents the non-exclusive license to archive, make accessible, and display my thesis in whole or in part in all forms of media, now or hereafter now, including display on the World Wide Web. I understand that I may select some access restrictions as part of the online submission of this thesis. I retain all ownership rights to the copyright of the thesis. I also retain the right to use in future works (such as articles or books) all or part of this thesis.

Joseph Adam Schultz April 12th, 2016

Changes in VGLUT1 Synaptic Connectivity and Presynaptic Inhibition Following Nerve Crush

by

Joseph Adam Schultz

Francisco Alvarez, Ph.D.
Adviser

Neuroscience and Behavioral Biology

Francisco Alvarez, Ph.D.
Adviser

Yoland Smith, Ph.D.

Committee Member

Shawn Hochman, Ph.D.

Committee Member

Arthur English, Ph.D.

Committee Member

2016

Changes in VGLUT1 Synaptic Connectivity and Presynaptic Inhibition Following Nerve Crush

By

Joseph Adam Schultz

Francisco Alvarez, Ph.D.

Adviser

An abstract of
a thesis submitted to the Faculty of Emory College of Arts and Sciences
of Emory University in partial fulfillment
of the requirements of the degree of
Bachelor of Sciences with Honors

Neuroscience and Behavioral Biology

2016

Abstract

Changes in VGLUT1 Synaptic Connectivity and Presynaptic Inhibition Following Nerve Crush
By Joseph Adam Schultz

Group IA afferents innervate muscle spindles in the periphery and form monosynaptic connections with motoneurons (MNs) in the spinal cord. This connection generates the stretch reflex, which is susceptible to changes following nerve injury. After nerve transection 60% of regenerated MNs lose their stretch-evoked EPSPs, resulting in a near complete loss of the stretch reflex. In contrast, after nerve crush, stretch-evoked EPSPs are maintained in regenerated MNs and recorded muscle forces during the stretch exceed 140% baseline values. This difference between crush and transection might be partially explained by better preservation of IA afferent connections on MNs and also by a decrease in the amount of presynaptic inhibitory control that modulate these connections. To test these hypotheses we used immunoreactivity of vesicular glutamate transporter 1 (VGLUT1) and the 65 kDa isoform of glutamic acid-decarboxylase (GAD65) as markers of IA afferent contacts and presynaptic inhibition, respectively, and analyzed their numbers and characteristics on MNs that are regenerating (21 days post crush) or have reinnervated muscle (3 months) after nerve crush. The left tibial nerves of adult Wistar rats were subjected to a crush nerve injury while the MNs innervating the medial gastrocnemius muscle were retrogradely labeled with cholera toxin b (CtB, Alexa Fluor 555). Spinal cords were extracted, sectioned, processed for triple-color fluorescence (CtB-red, VGluT1-green and GAD65-infrared) and imaged with confocal microscopy. The dendritic arbors of individual MNs were then digitally traced, and VGLUT1 and GAD65 terminals plotted on them and counted. Our results show a slight loss of dendritic VGLUT1 terminals at both 21 day and 3 month post-crush (respectively: -33%, $p<0.01$ and 26%, $p<0.05$). This contrasts with the over 60% losses estimated in the same region of dendrite after transection. In addition, we found a significant decrease in the number of GAD65 terminals per VGLUT1 terminal in both 21 day and 3 month post-crush animals (respectively: -32%, $p<0.01$ and -20%, $p<0.05$). These results support the hypothesis that better preservation of IA afferent connections and a loss of presynaptic control could be partially responsible for the maintenance of the stretch reflex and the increase in reflex forces after nerve crush.

Changes in VGLUT1 Synaptic Connectivity and Presynaptic Inhibition Following Nerve Crush

By

Joseph Adam Schultz

Francisco Alvarez, Ph.D.

Adviser

A thesis submitted to the Faculty of Emory College of Arts and Sciences
of Emory University in partial fulfillment
of the requirements of the degree of
Bachelor of Sciences with Honors

Neuroscience and Behavioral Biology

2016

Acknowledgements

I would like to thank the Neuroscience and Behavioral Biology Department at Emory University as well as the Atlanta NET/Work program for creating the opportunity for me to complete this honors thesis. I would also like to give thanks to Dr. Smith, Dr. Hochman, and Dr. English for being members of my committee.

To Dr. Alvarez, I extend special thanks for his constant support throughout the project. I am forever grateful for the opportunity to have pursued this line of research during the last two years in his laboratory, for the mentorship he has provided, and for one of the most valuable and intellectual scientific experiences I have had at Emory.

I would like to thank Travis Rotterman for two years of daily mentorship. For teaching me the ins-and-outs of lab work, providing feedback on numerous documents and presentations, helping ensure the success of my thesis and defense, and always trying to prevent me from over-stressing, I am eternally thankful.

I would also like to thank my colleagues and friends in the lab: Dr. Ron Griffith, Dr. JoAnna Anderson, Dr. Laura Gomez, Erica Akhter, and Alicia Lane. Thank you all for always making me feel at home in lab, for all the interesting conversations we have had, and for all the small but wonderful events and celebrations.

I am also grateful to Dr. Timothy Cope, Paul Nardelli, Laurie Goss, and the other members of the Cope laboratory for performing the animal care and many surgeries involved in this project. Without their assistance, this project would not have been possible to complete in these two years.

Finally, a huge thank you to my friends, who have provided relief and support during the most stressful moments of this project, my father, who always reminds me to pursue my goals, and my mother, who has always encouraged me to do my best in everything that I do.

Table of Contents

Introduction

Peripheral nerve injuries may arise from a variety of trauma ranging from automobile accidents to gunshot wounds to lacerations. These injuries annually affect in excess of 200,000 people in the United States (Taylor et al., 2008), and as many as 90% will never recover full motor or sensory function (Portincasa et al., 2007; Scholz et al., 2009). Even if successful peripheral axonal regeneration is achieved following surgical repair, persistent motor deficits remain. For example, deficits in slope walking have been shown to persist even after successful reinnervation of peripheral targets (Abelew et al., 2000; Maas et al., 2007; Sabatier et al., 2011). These deficits most likely arise from disruptions in proprioceptive feedback that are not necessarily associated with misdirection of axons in peripheral nerves during recovery. One potential explanation for the permanency of these deficits is the plasticity of spinal cord circuitry after nerve injury (Navarro, 2009). In the case of peripheral nerve transection, in which the axons of the nerve are completely severed, these changes result in the loss of the stretch reflex mediated by the direct connections of IA stretch-responsive muscle sensory afferents on motoneurons (MNs). These disruptions are well documented, and it is known that MNs that regenerate and reinnervate muscles after complete nerve transections lack responses to mechanical stimulation of the stretch reflex (Cope et al., 1994; Huyghues-Despointes et al., 2003; Haftel et al., 2005; Bullinger et al., 2011). The loss of MN responses to stretch is explained, at least in part, by the retraction of axons from IA afferents from the ventral horn. This was demonstrated by two studies in our lab in which we found a permanent loss of approximately 60% of excitatory inputs from IA afferents, as defined by synapses containing vesicular glutamate transporter 1 (VGLUT1), connecting to MNs up to a year after the injury and

well after regeneration in the peripheral nerve and muscle reinnervation are completed (Alvarez et al., 2011; Rotterman et al., 2014).

Interestingly, MNs seem to recover their ability to respond to IA afferent monosynaptic excitatory postsynaptic potentials (EPSPs) evoked via electrical stimulation (Mendell et al., 1995; Haftel et al., 2005; Bullinger et al., 2011). Indeed, electrical measures of the monosynaptic stretch reflex, such as the H-reflex, demonstrate a partial or even complete recovery (Valero-Cabre and Navarro, 2001; English et al., 2007). The discrepancy between stretch-evoked and electrically-evoked IA afferent-MN monosynaptic EPSPs is not fully resolved.

In contrast to the complete absence of the stretch reflex observed after complete nerve transection, one study performed by Prather et al. (2011) indicates the presence of a supranormal stretch reflex in cats that have undergone peripheral nerve crush. This type of injury is fundamentally different from transection in that the continuity of the endoneurial tubes that will guide regenerating axons to their targets is maintained following injury resulting in facilitation and greater specificity of targeted reinnervation (Madison et al., 1996; Nguyen et al., 2002). Interestingly, 70% of IA afferents successfully reinnervate the muscle spindles of these cats after nerve crush (Gallego et al., 1980) and Prather and colleagues (2011) reported a 70% preservation of stretch-evoked EPSPs in MNs. This is different from the large depression of IA stretch-evoked EPSPs that occurs after complete transection of the same nerve (Bullinger et al., 2011). These results predict that VGLUT1 synapses should be better preserved anatomically after nerve crush compared to full nerve transections.

Increased synaptic preservation is certainly a pre-requisite for the results described in Prather and colleagues (2011); however, additional factors need to be considered to explain why dynamic stretch reflex forces were increased by 145% or greater after nerve crush. This increase

in reflex forces can, potentially, be explained by alternative changes in spinal cord circuitry. For example, presynaptic inhibition of cutaneous sensory afferent mechanoreceptor synapses is reduced in the dorsal horn following peripheral nerve injury, and this is associated with a loss of GABAergic synapses (Horch and Lisney, 1981; Castro-Lopes et al., 1993; Moore et al., 2002). The effect of crush injury on presynaptic inhibition of ventral proprioceptive IA afferents is much less clear (Enriquez et al., 1996; Enriquez-Denton et al., 2004) and has not yet been analyzed at the structural level. Indeed, one potential explanation for the increased stretch-reflex is either a loss or a disorganization of presynaptic GABAergic terminals.

We hypothesized that following crush injury i) there is a better preservation of IA afferent synapses than after complete transection and ii) GABAergic presynaptic control of remaining IA afferent contacts is diminished, contributing to an exaggerated stretch response. Our results suggest that IA afferent contacts, as defined by the amount of VGLUT1 immunoreactive synapses contacting the MN dendrites and somata, are better preserved following nerve crush than complete nerve transection. Furthermore, immunocytochemically, presynaptic boutons on IA afferents can be defined by immunoreactivity to the 65kda isoform of glutamic decarboxylase (GAD65), on remaining IA afferent VGLUT1-IR synapses on MNs (Hughes et al., 2005; Betley et al., 2009); thus a decrease in the amount of GAD65-IR terminals contacting individual VGLUT1 terminals would suggest a decrease in the amount of GABAergic presynaptic control of MNs. This may provide one possible explanation for the phenomena reported by Prather and colleagues.

Methods

All animal care, nerve surgeries, and terminal experiments were performed at Wright State University and approved by the institutional laboratory animal use committee at Wright State University. Collected tissues were sent to Emory University for post-processing.

Nerve injury and injections: Adult female Wistar rats (225-300g) were anesthetized with isoflurane until the animal achieved a surgical plane of anesthesia (induction 4-5%; maintenance 1-3%, both in 100% O_2). The tibial nerve (TN) was exposed at midthigh by a midline posterior incision (~1.5cm) through the skin and underlying connective tissue of the left hindlimb. The TN was then crushed with fine #5 forceps for 10s. After washing with 0.9% sterile saline, the wound was closed in layers and the animals were removed from anesthesia. A subcutaneous injection of buprenorphine (0.1mg/kg) was delivered immediately and every 12 hours after surgery prophylactically to alleviate any possible pain and distress for 48 hours. Signs of pain and distress (lethargy, vocalizations, weight loss, absence of grooming) were closely monitored but not observed in any animals. One week prior to being sacrificed, the MG muscle of the left leg was exposed again and 1-5% CtB-555 (Invitrogen) was injected in four or five 2 to 5µl injections in order to visualize the dendritic arbor and somata of MNs that reinnervated the MG during analysis of VGLUT1 and GAD65 contact distributions.

Histology and immunocytochemistry: The animals were sacrificed and transcardially perfused with 4% paraformaldehyde in 0.1M phosphate buffer at 21 days (before nerve regeneration and muscle reinnervation) or 3 months (after nerve regeneration and muscle reinnervation) following the nerve crush. Spinal cords were collected and post-fixed overnight. Lumbar regions 4 and 5 (L4-L5) were extracted and 50µm thick sections were collected from a freezing sliding microtome. Sections were washed 3x for 10 minutes in 0.01M PBS with 0.3%

triton and then blocked in 10% normal donkey serum for 1 hour. Sections were then incubated in rabbit anti-VGLUT1 (1:1000, Synaptic Systems) and mouse anti-GAD65 (1:200, Developmental Hybridoam Bank) antibodies for 24 hours at room temperature. Primary antibodies were washed off by 10 minute washes in 0.01M PBS with 0.3% triton, which was repeated 3x before being placed in a mixture of anti-rabbit and anti-mouse IgG secondary antibodies each tagged to different fluorochromes (1:100, FITC and Dy647, Jackson ImmunoResearch) to distinguish the different immunoreactivities.

Confocal imaging and neuron reconstruction: Sections from each animal were imaged first at low (20x, N.A. 0.70) and then at high (60x, N.A. 1.35, oil immersion) magnification in an Olympus FV1000 confocal microscope. Large CtB-immunoreactive (CtB-IR) profiles were randomly sampled from LIX motoneuron pools known to send axons in the MG nerve. Each CtB-IR profile and associated synaptic varicosities were imaged through series of confocal images separated by 0.5μm *z*-steps. These images were then transferred to and reconstructed in Neurolucida (MicroBrightField). The position of each VGLUT1-IR synapse was labeled using a "marker" (filled circle) that was then "attached" to its dendritic position. GAD65-IR synapses in contact with VGLUT1-IR synapses were labeled with a different marker (inverted triangle). Cell bodies were reconstructed through a series of contours traced in each optical plane. VGLUT1-IR terminals contacting the soma and the GAD65-IR terminals in contact with them were labeled with their own unique markers (respectively: filled triangle and empty square). All images were coded and counts were performed blinded to the condition of the animal.

Quantification: Traced neurons and attached synaptic markers were analyzed using Neuroexplorer (v10.0, MicroBrightField). Total length (pathlengths of all dendritic branches added) and overall surface of the combined dendrites as well as the surface of the cell body were

measured (see Table 1). First, the distribution of VGLUT1-IR synapses was analyzed by obtaining the following two measurements: (1) Overall VGLUT1 terminal densities were calculated by dividing the total number of terminals by the total dendritic length (linear), total dendritic surface, or cell body surface area. (2) Sholl analysis was used to examine VGLUT1 terminal distributions along the dendrites. For this purpose, a series of concentric nested spheres were placed around the cell body to segment the dendritic arbor in 50μm bins of incremental radial distance from the center of the cell body. Linear and surface densities of VGLUT1 terminals within each bin were then calculated. Next, changes in the distribution of GAD65-IR terminals on VGLUT1 terminals were analyzed using two separate measurements. (1) The percentage of VGLUT1 terminals receiving contact from GAD65 terminals was calculated for both dendritic and somatic VGLUT1 terminals. (2) The density of GAD65-IR terminals was measured by calculating the average ratio of GAD65 to VGLUT1 terminals (total GAD65 terminals/total VGLUT1 terminals) for both dendritic and somatic VGLUT1 terminals. Using these methods, we analyzed 40 MNs in each of three experimental groups (control, 21 day, 3 month), sampling 10 MNs per animal in each group (n=4 animals per group).

Surface-to-surface analysis: The initial observations suggested that GAD65-IR terminals could be smaller after injury; thereby raising the possibility that not only the number, but also the amount of surface covered by GAD65-IR boutons on VGLUT1-IR IA afferent terminals was diminished. To analyze the percentage of surface contact between both boutons, confocal images were loaded into IMARIS (Bitplane), a 3D image analysis program, to calculate the amount of GAD65 surface area in contact with single VGLUT1 terminals. Using this software, we obtained 3D renderings of individual randomly selected VGLUT1-IR terminals (10 terminals per condition; 1 animal per condition) and of the GAD65 terminals contacting them. Synaptic

boutons were "segmented" for the image using fluorescent thresholding. In this method the intensity of the fluorescent signal is used to outline the bouton and produce a surface rendered object from which we can determine the size of the bouton and its surface area. Thresholds for this process were determined based on the first control terminal examined, and then applied to all further sampled boutons using the same conditions. These thresholds were only adjusted in six cases, in which the fluorescence was not strong enough on the inner portion of the synapse to produce an image. We then used the built-in software analysis tools of IMARIS to compute the total surface area of each rendered VGLUT1 terminal, and used a custom MATLAB script to calculate the surface area of the VGLUT1 terminal covered by GAD65-IR synapses. For this determination we defined the surfaces of the GAD65 and VGLUT1 bouton to be in close contact if there was no separation in space between the two surfaces. From these measurements we calculated the percentage of VGLUT1 terminal surface area contacted by GAD65 terminals.

Statistical analyses: All statistical tests were made using SigmaPlot 12.3 (Systat). When possible, we used one-way analysis of variance (ANOVAs) to compare VGLUT1 dendritic linear density, dendritic surface area density, and somatic density between control, 21 day crush, and 3 month crush animals. Bonferroni's post-hoc analysis was used to determine significant differences between the different experimental groups and control averages. This analysis was also used to compare the percentage of VGLUT1 terminals receiving contact from GAD65-IR terminals, the ratio of GAD65-IR terminals per VGLUT1 terminals, the size of both VGLUT1 and GAD65 terminals, and the percentage of VGLUT1 terminal surface area contacted by GAD65 terminals. If normality failed due to small sample sizes, a non-parameteric rank sum test (Dunn's) was executed to define any significant differences. Alpha value was set to 0.05.

Results

VGLUT1 Terminals are Minimally Lost in Proximal Dendrites Following Nerve Crush.

To quantify VGLUT1 terminals in contact with the soma and proximal dendrites of motoneurons, CtB was injected in the MG muscle to retrogradely label α-MN cell bodies and proximal dendrites in lamina IX of the spinal cord (Alvarez et al. 2011). CtB-IR cell bodies from control and crush animals, 21 day or 3 months after injury (n=4 in each group; 10 MNs per animal) were imaged at high magnification (Fig. 1) and reconstructed with Neurolucida (Fig. 2) to estimate contact densities. One caveat of CtB labeling is its limited diffusion once it reaches the cell body. This limits labeling to the most proximal dendrites, and the total length of dendrites labeled per cell in this study never exceeded 1000 μm (Table 1). Despite this limitation, previous reports have indicated that 75% of all VGLUT1 contacts in uninjured animals are located within the first 550 μm of the dendritic arbor (Rotterman et al., 2014). Therefore, we are confident that the results are representative of the overall VGLUT1 population.

Table 1: Somatic and dendritic surfaces and lengths sampled in CtB-labeled motoneurons.

Values are means ± SD.

	Controls (n=4)	21 Day Crush (n=4)	3 Month Crush (n=4)
Soma			
Surface Area (μm^2)	6150 ± 525	6163 ± 591	6232 ± 525
Dendrites			
Length (µm)	802 ± 59	837 ± 155	774 ± 87
Surface Area (μm^2)	13068 ± 2473	11392 ± 3349	10999 ± 1371

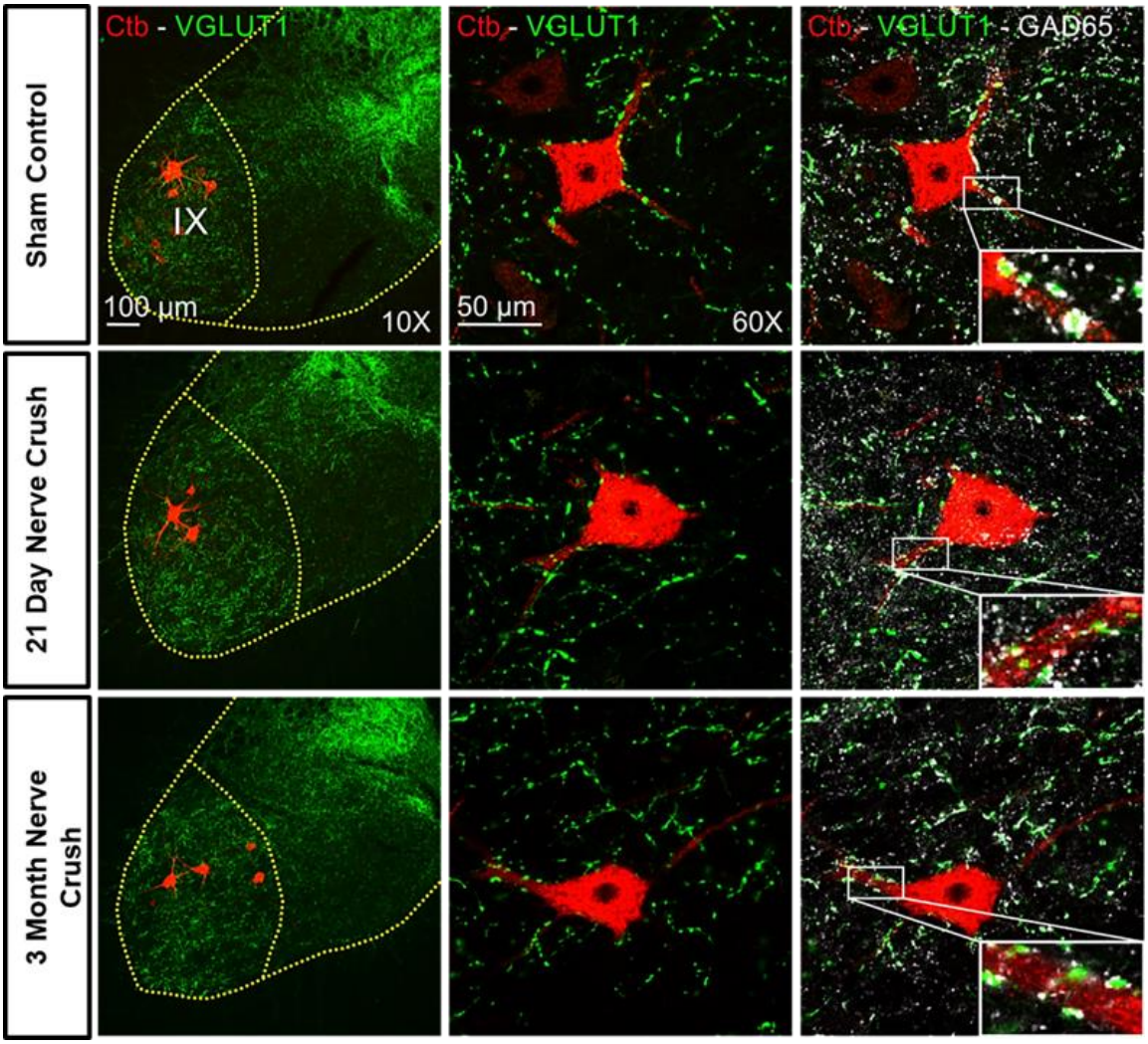

Figure 1: Confocal images of MG motoneurons residing in the motor pool in lamina IX. *Left*: Low magnification images (10x) of lumbar spinal cord sections with motoneurons retrogradely labeled with cholera toxin subunit b (CtB) conjugated to an Alexa Fluor-555 fluorochrome. Sections were subsequently immunolabeled for VGLUT1 (IA afferents) in FITC (green) and GAD65 (GABAergic inhibitory synaptic marker) in Dy647 (white). *Middle*: high magnification images (10 sections at 0.5µm z-steps, 60x) of CtB-labeled MG motoneurons in control, 21 day post-injury, and 3 month post-injury animals (top to bottom). *Right*: same images as middle column, but with GAD65 immunofluorescence added. Insets show the effects of nerve crush on dendritic VGLUT1 and GAD65 contacts.

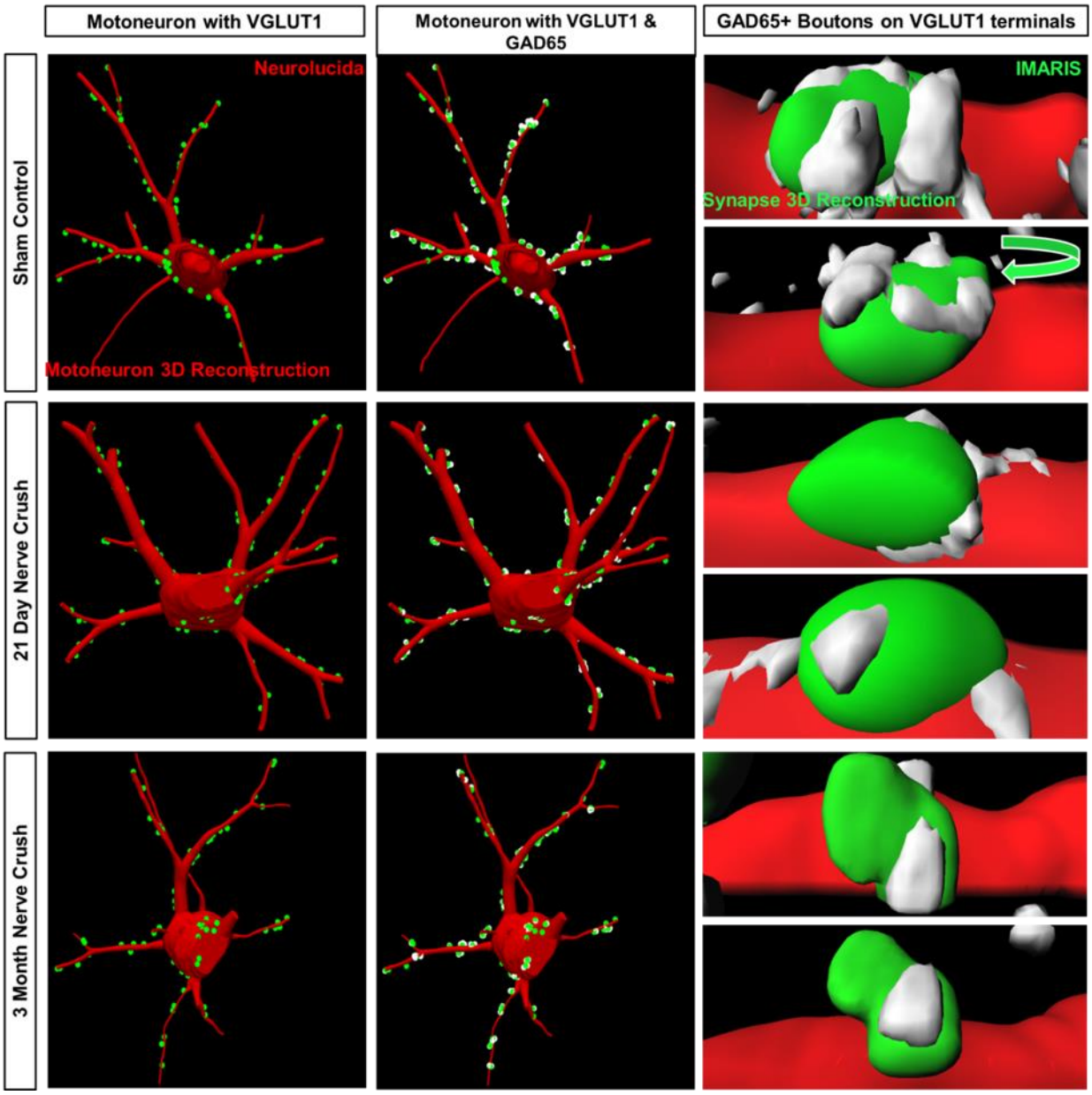

Figure 2: Examples of Neurolucida reconstructions MG motoneurons (left two columns) and IMARIS reconstructions of individual VGLUT1 terminals and the GAD65 terminals contacting them (right column). In all images, red represents an area labeled by CtB (motoneuron) while green represents VGLUT1 immunofluorescence and white represents GAD65 immunofluorescence.

Estimations of VGLUT1 dendritic linear density (VGLUT1 density per 100µm, Fig. 3A) revealed a significant depletion following crush injury in the 21 day group (33%, $p<0.01$; control

average=12.5±0.8, ±SD). Despite ample time for successful muscle reinnervation, these contacts did not recover at the later post-injury time, and the 3 month group still exhibited a significant depletion from controls in VGLUT1 dendritic linear density (-26%, $P<0.05$). Surface area density (VGLUT1 density per 100µm^2) of VGLUT1 contacts was also found to be depleted in both the 21 day and 3 month groups (respectively: 21% and 19%; Fig. 3B).

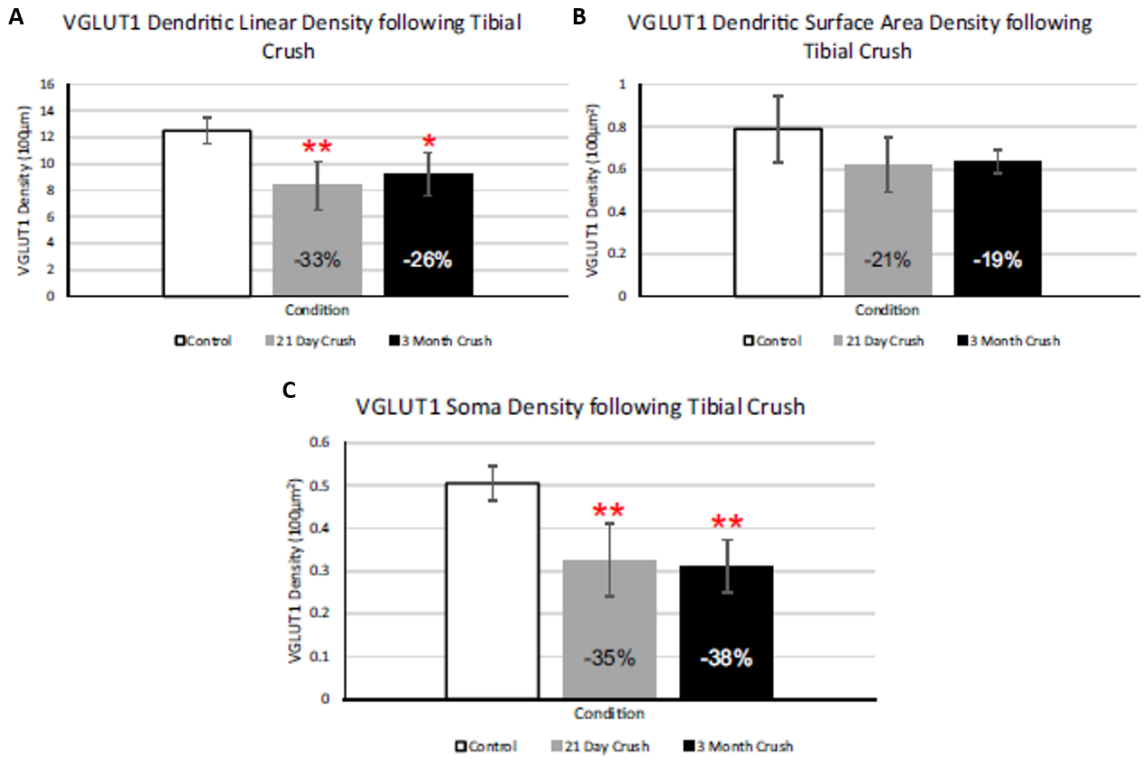

Figure 3: Quantitative analysis of changes in VGLUT1-IR contacts on the dendrites and somata of MG motoneurons at either 21 days or 3 months after tibial nerve crush. Each bar represents the group averages (n=4 animals/group; 40 MNs analyzed per group) of all animals sampled at a particular post-injury time point. Single asterisk indicates P<0.05, double asterisk indicates P<0.01, all statistical analyses are one-way ANOVA with Bonferroni post-hoc analysis, %s indicate percent depletion from control averages. ***A***: average VGLUT1-IR linear densities (amount of VGLUT1-IR contacts per 100µm) on the dendrites of CtB-labeled MG motoneurons. The control group was significantly different from both nerve injury groups. Although the 3 month group was less depleted than the 21 day crush group, this

difference was not significant. ***B***: average VGLUT1-IR surface densities (amount of VGLUT1-IR contacts per 100μm^2) on the dendrites of CtB-labeled MG motoneurons. Although depletions at both post-injury time points are present, there is no significant difference between both lesioned groups and controls. ***C***: average VGLUT1-IR soma densities (amount of VGLUT1-IR contacts per 100μm^2 of somatic surface area). Depletions were observed at both post-injury time points, and the control group was significantly different from both groups.

However, depletions in VGLUT1 surface densities on dendrites did not reach statistical significance. This is likely due to decreases in dendritic surface area after injury which varies from animal to animal and may be due to variable thinning of proximal dendrites in regenerated MNs or lesser uptake of the retrograde tracer CtB that might not fill the thickness of the dendrite as completely.

Similar depletions were found for VGLUT1 terminals in contact with the cell bodies of MNs. Controls received an average of 0.5±0.03 VGLUT1 contacts per 100μm^2 (Fig. 3C) and VGLUT1 soma density was significantly reduced in both the 21 day and 3 month groups (respectively:-35%, $p<0.01$ and 38%, $p<0.01$). The size of these depletions, which range from 19% to 38%, is much less substantial than the loss reported after nerve transection, in which approximately 60% of VGLUT1-IR contacts were lost in the same dendritic regions (Alvarez et al., 2011). Furthermore, the magnitude of these depletions aligns well with results from Prather et al., (2011) in which a 30% loss in muscle stretch evoked postsynaptic potentials, or strEPSPs, was recorded.

We then examined whether changes to the proximo-distal distribution of synaptic contacts may be a consequence of nerve crush injury. Analysis of the distribution of VGLUT1 contacts via Sholl analysis revealed that there was a significant decrease (Fig. 4, $p<0.05$) in the

linear density of VGLUT1 contacts in all bins of the 3 month crush group. A general decrease in linear density across the bins of the 21 day crush group was also present, but this reduction did not reach significance, perhaps due to increased variability caused by reductions in the sample size due to segregation of the data into different bins. Percent losses in VGLUT1 contacts were calculated in order to better visualize the size of the depletion bin-by-bin. In the 21 day group, the averaged percent losses amounted to 35%, 24%, and 12% in the soma, 50µm, and 100µm bins, respectively, and 38%, 35%, and 28% in the 3 month group. This pattern of depletion indicates that the loss of VGLUT1 contacts is evenly distributed throughout the most proximal dendrites. This is notably different from transection, in which the vast majority of the loss occurs on the soma and within the first 50µm of the dendrites. As in the overall data, the depletion after crush is much smaller than after transection of the same nerve in each individual Sholl bin.

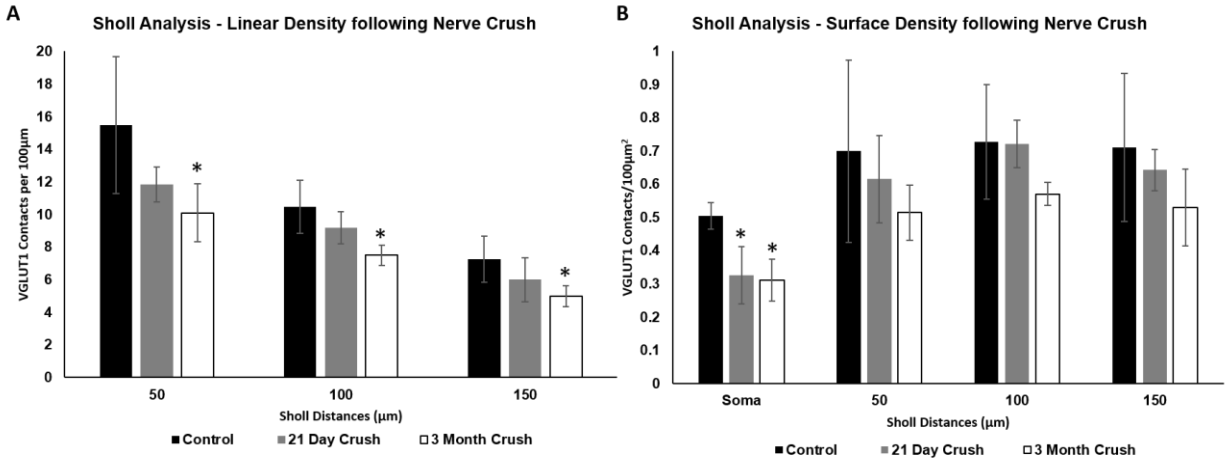

Figure 4: Quantitative analysis of the proximo-distal distribution of IA afferent contacts via VGLUT1 densities on the dendrites of MG motoneurons after peripheral nerve crush. Each bar represents the group averages (n=4 animals/group; 40 MNs analyzed per group) of all animals sampled at a particular postinjury time point. Single asterisk indicates $P<0.05$, all statistical analyses are one-way

ANOVA with Bonferroni post-hoc analysis. ***A***: Average VGLUT1 linear density (VGLUT1-IR contacts per 100μm) was depleted on all three Sholl bins from 3 month animals (white bars) compared to controls (black bars). All depletions in this group were found to be statistically significant. Although depletions were observed in all three bins from 21 day animals (grey bar), none of these depletions were significantly different from controls. ***B***: Average VGLUT1 surface density (VGLUT1-IR contacts per 100 μm^2) was slightly depleted in all groups and bins of the dendrites except the 100μm Sholl bin from the 21 day animals. However, these depletions were statistically significant only on the soma.

Presynaptic GABAergic Control of VGLUT1 Contacts is Reduced Following Nerve Crush

The better preservation of VGLUT1 synapses following nerve crush compared to complete transection provided some insight into the mechanism of the phenomenon reported by Prather et al in 2011; however, this alone does not fully account for the enhancement of reflex forces after nerve crush. In order to examine one additional mechanism that may contribute to such an enhancement, we examined the effects of nerve crush on GABAergic, presynaptic control using GAD65 immunoreactivity as a marker of presynaptic (P) boutons (Fig. 5).

The percentage of VGLUT1-IR terminals receiving presynaptic inhibition in controls (defined by receiving contacts from GAD65-IR P boutons) was 86.9% on both the dendrites and soma (Fig. 5A & B). In the 21 day crush group there was a small, but significant ($P<0.05$), 14% reduction in the percentage of dendritic VGLUT1 terminals receiving any GAD65-IR contact (Fig. 5A). Decreases in this measure were non-significant in the 3 month group and were non-significant when somatic VGLUT1 terminals were examined at either time point (Fig. 5B).

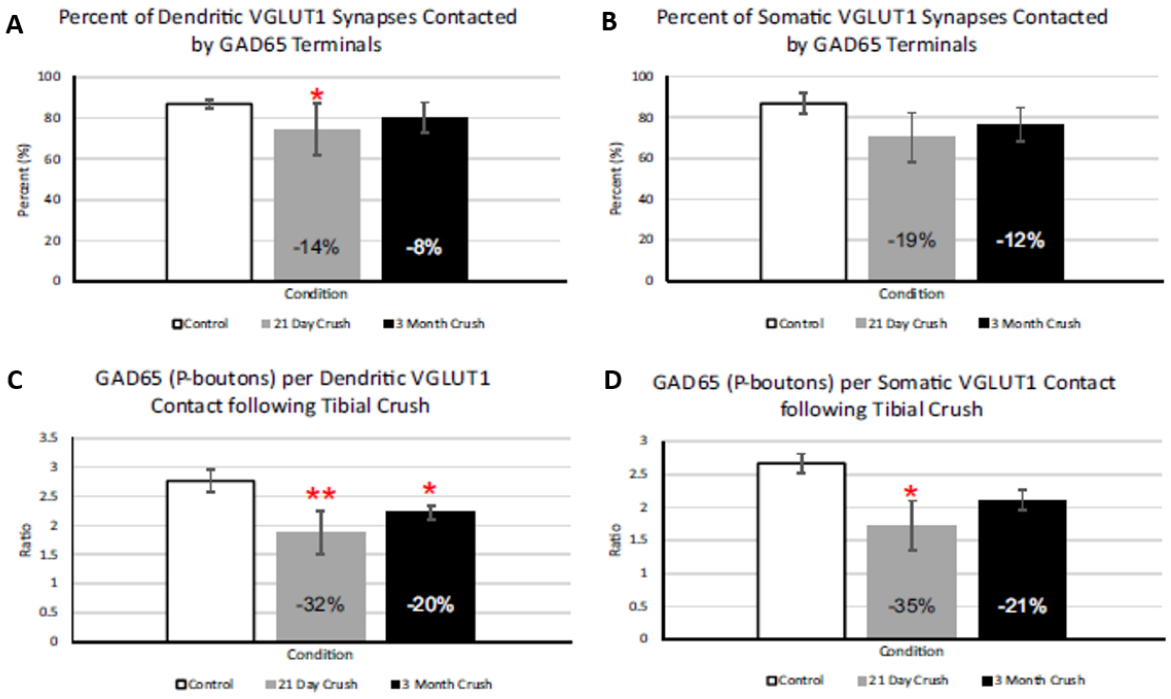

Figure 5: Quantitative analysis of changes in GAD65-IR terminals contacting VGLUT1-IR terminals on the dendrites and somata of MG motoneurons at either 21 days or 3 months after tibial nerve crush. Each bar represents the group averages (n=4 animals/group; 40 motoneurons analyzed per group) of all animals sampled at a particular postinjury time point. Single asterisk indicates $P<0.05$, double asterisk indicates $P<0.01$, all statistical analyses are one-way ANOVA with Bonferroni post-hoc analysis, %s indicate percent depletion from control averages. ***A-B***: comparison of the percentages of VGLUT1-IR terminals receiving any amount of contact from GAD65-IR terminals. ***A***: the percentage of VGLUT1-IR terminals receiving presynaptic control was depleted at both postinjury time points. However, this depletion was only significant in 21 day crush animals (grey bar) compared to controls. ***B***: although depletions in the percentage of somatic VGLUT1-IR terminals receiving presynaptic control was depleted at both postinjury time points, neither of these groups were significantly different from controls. ***C-D***: comparison of the amount of GAD65-IR terminals contacting VGLUT1-IR terminals. ***C***: in contrast to the percentages observed in A and B, the average ratio of GAD65-IR terminals per dendritic VGLUT1-IR terminal was significantly reduced at both postinjury time points compared to

controls. ***D***: the average ratio of GAD65-IR terminals per somatic VGLUT1-IR terminal was also reduced at both postinjury time points. However, only the reduction in the 21 day crush animals was significantly different from controls in this case. Although there appears to be a recovery of GAD65-IR terminals by 3 months for both dendritic and somatic contacts, the differences between post-injury groups was not significant in either case.

There was, however, a difference in the number of GAD65 boutons per VGLUT1 terminal. In VGLUT1 terminals on dendrites of the combined control group we found an average of 2.8±0.2 GAD65 boutons per VGLUT1 terminal (Fig. 5C). Compared to the control value, both the 21 day crush and 3 month crush groups had significant reductions (respectively: -32%, $p<0.01$ and -20%, $p<0.05$) in the number of GAD65 boutons per dendritic VGLUT1 terminal. A similar decrease was found on VGLUT1 terminals on MN somas of the 21 day crush group (-35%, $p<0.05$; control average=2.7±0.2; Fig. 5D). However, despite a 21% decrease on the somatic VGLUT1-IR terminals in the 3 month crush group, this reduction did not reach significance. Taken together, these results indicate that IA afferent synapses may not lose all presynaptic inhibitory control following nerve crush, but the amount that remains is significantly diminished in both animals that are at initial stages of regeneration (21 days) or that have completed regeneration and muscle reinnervation (3 months).

Surface Area Reconstructions of VGLUT1 and GAD65 Terminals

In our images we noticed that GAD65-IR P-boutons associated with VGLUT1-IR synapses on regenerated MNs were smaller than in control. Another possibility to explain the enhanced reflex is that the total GAD65+ bouton surface area contacting VGLUT1 synapses has decreased in overall coverage, perhaps suggesting a weakening of the presynaptic bouton. In order to examine this, we used IMARIS 3D imaging software to digitally render the surfaces of individual VGLUT1 and GAD65 terminals. We then used a MATLAB script to calculate the

percentage of VGLUT1 surface area covered by GAD65 surface area and compared this between all three conditions.

In order to examine the effects of nerve crush on GAD65 terminal size, we first needed to ensure that the size of VGLUT1 terminals we were selecting remained consistent throughout the various conditions since the number of GAD65 P-boutons varies with the size of the IA afferent. Figure 6A shows that VGLUT1 terminals selected in all three groups were similar in size. Having confirmed this, we then examined whether GAD65 terminals decrease in size following nerve crush injury. Control GAD65 terminals averaged a surface area of 12.21μm^2±6.8 (n=10; Fig. 6B). GAD65 terminals did trend towards a reduction in size. In the 21 day crush group, the average surface area of GAD65 terminals was 7.21μm^2±6.1 (n=10). This trend towards decrease was still present in the 3 month group where averages were equal to 6.43μm^2±4.3 (n=10). However, this trend did not reach significance via one-way ANOVA (p=0.073), perhaps due to large amounts of variability associated with small sample size and indicated by low statistical power (0.347). Despite a lack in significance, this trend towards a decrease in size may indicate that the decrease in presynaptic GABAergic inhibition might not be limited to a decrease in the number of terminals, but could also be a result of decreasing surface area in contact with the VGLUT1 terminals of the remaining inhibitory synapses.

We examined the percentage of each VGLUT1 terminal's surface area that was contacted by GAD65 terminals (Fig. 6C). Control VGLUT1 terminals were covered by GAD65 contacts on 36.7% of their total surface area. In the 21 day crush group, the percent surface area coverage was about half of that calculated in controls (18.8%). This trend continued in the 3 month group where percent coverage was also equal to around half of the control value (19.1%). Despite these large differences, no significant difference was found because of small sample sizes to date.

These results, however, warrant further investigation into whether a change in the size of terminals, resulting in a decrease in the area available for vesicle release may provide further explanations for the results reported by Prather et al., (2011).

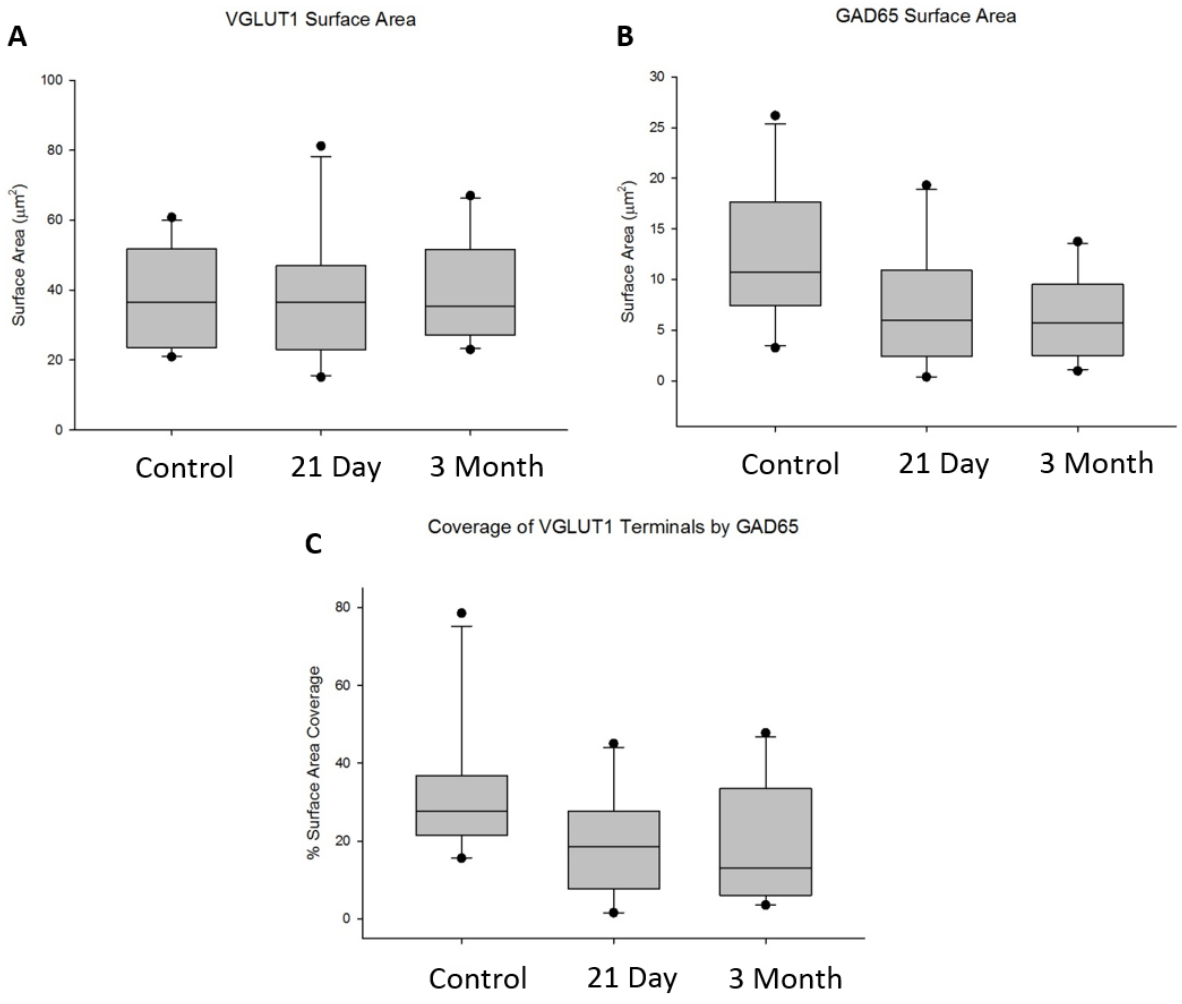

Figure 6: Quantitative analysis of changes in the size of VGLUT1 and GAD65 terminals. Each box plot represents data collected from the analysis of 10 individual VGLUT1 terminals in 1 animal from each group. ***A***: VGLUT1 terminals were chosen to be of similar size in order to make a more valid comparison of changes in the size of GAD65 terminals. ***B***: the average size of GAD65 terminals contacting examined VGLUT1 terminals was reduced at both postinjury time points. However, these reductions did not reach statistical significance ($P<0.07$), perhaps as a result of low statistical power (0.347). ***C***: the percentage of VGLUT1 surface area directly contacted by GAD65 terminals (% surface area coverage) was also reduced in both postinjury groups. However, this data was not significant either. In this case, the sample failed to achieve normality, indicating the need for a larger sample size.

Discussion

One major finding of this study indicates that the loss of IA afferent input on the soma and dendritic arbor of MG MNs following tibial nerve crush (~30%) is less severe than the losses reported after complete nerve transection (~60%, Alvarez et al., 2011) and frequently does not reach statistical significance. Notably, the reduction in IA synapses demonstrated here aligns well with the functional data demonstrated by Prather and colleagues, in which they reported a 70% preservation in the strength of strEPSPs after nerve crush.

The more mild deficits after crush compared to transection parallel higher rates of successful reinnervation of the appropriate peripheral targets, probably due to a lack of disruption to the endoneurial tubes in this injury paradigm (Madison et al., 1996; Nguyen et al., 2002). It is not fully known how different types of injuries in the periphery can trigger different types of synaptic plasticity centrally inside the spinal cord. One potential explanation involves the strength of the neuroinflammatory reaction. Preliminary data from our laboratory indicates that crush induces a much milder microglia response than cut. We think that the robust microglia response is important in synaptic displacement and degradation. Therefore, if the microglia response is much lower in crush, it is possible that this leads to better retention of existing connections after injury. Our results suggest that the mild functional deficits witnessed in nerve crush may be a result of a better preservation of the synaptic contacts of IA afferents onto MNs. Despite these results, no solid connection between functional deficits and the structural results shown here can be made at present because there is no functional data in the rat, and those studies that examined functional deficits in the stretch reflex after nerve crush were performed in the cat. For this reason, it will be important to investigate if these structural changes found in the rat result in an enhanced strEPSP, as was previously reported in the cat.

The other major finding of this study is an apparent reduction in the amount of GABAergic presynaptic control contacting each individual IA afferent. It is uncertain how peripheral nerve crush affects presynaptic inhibition. Our results align closely with the findings of Horch and Lisney (1981), in which nerve crush seemingly resulted in a decrease in the level of presynaptic inhibition in cutaneous mechanoreceptors. However, Enriquez-Denton et al. (2004) suggest that presynaptic inhibition on IA afferents is unaffected by nerve crush, and that the level of presynaptic inhibition, measured in terms of excitability thresholds of the central terminations of IA afferents, is not significantly different between injured animals and uninjured controls. Interestingly, earlier work from the same group reached a slightly different conclusion, but this time measuring primary afferent depolarization (PAD) in IA afferents (Enriquez et al., 1996). In this study, IA afferents showed, in addition to normal PAD after stimulation of muscle afferents, abnormal PAD after stimulation of the reticular formation (RF) of the brainstem or of cutaneous sensory afferents. PAD responses following activation of RF or skin sensory afferents is typical of IB fibers and not IA fibers. These results suggest that there may be a reorganization of inhibitory circuits following peripheral crush injury (Enriquez et al., 1996). A change in modulation might reflect recruitment of different types of inhibitory presynaptic interneurons controlling a single IA afferent following injury, but the results do not provide enough information to determine the nature of this reorganization. Moreover, the data was obtained in cats and needs to be confirmed in rodents. One way in which this may be tested involves the use of a transgenic mouse line in which only a proportion of the GAD interneuron population expresses GFP. One study utilizing an animal model with mosaicism of GFP expression in GAD65 interneurons suggested that there is a rigid organizational pattern of presynaptic inhibition, in which all of the GAD65-IR terminals contacting a single VGLUT1-IR terminal

arise from a single, or few, interneurons within the pool (Hughes et al., 2005). This pattern might become disorganized following nerve injury and result in single IA afferent synapses receiving inputs from multiple inhibitory interneurons. In animal models where we induce genetically sparse labeling of presynaptic interneurons, we will expect in the control situation that VGLUT1 terminals are contacted by a single GFP+ interneuron, and each will have P-boutons that are either all or none expressing GFP. After nerve injury, this organization might be disrupted and P-boutons from different interneurons might now converge on single IA afferent terminals. If this is the case, GAD terminals on VGLUT1 terminals will become disorganized, so that both GFP+ and GFP- terminals contact the same VGLUT1 terminals. To test this hypothesis we have purchased an animal model to genetically induce sparse labeling of presynaptic GAD65 interneurons and their axons, and we are in the process of performing the necessary crosses to validate these expectations.

Regardless, the reduction in the number of GAD65-IR terminals demonstrated here may also provide a partial explanation for the supranormal stretch reflex forces witnessed by Prather and colleagues (2011).Similarly, the trend toward a reduction in coverage of VGLUT1 terminals by GAD65 boutons might also be a reflection of presynaptic weakening. Although the data involving the size of the GAD65 terminals does not reach significance, a trend towards decrease in the size of these terminals warrants further effort to increase the sample size such that the power of the statistical analyses could increase from 0.347 to at least 0.80. A decrease in the size of these terminals could indicate a decreased amount of area available for the release of synaptic vesicles. Synaptic bouton volume is known to be correlated with measures of a synapse's physiological strength, such as number and size of active zones and number of vesicles (Pierce and Lewin, 1994), and correlations between these values have also been demonstrated in IA

boutons, specifically (Pierce and Mendell, 1993). If nerve crush were to cause such a decrease in bouton volume, which seems likely based on our preliminary data, then it is possible that decreased synaptic efficacy may play a role in a potential reduction of presynaptic inhibitory control.

An investigation of changes in synaptic terminal size could also be investigated using electron microscopy (EM). We are currently in the process of optimizing these experiments, and have prepared samples from an uninjured rat in which MG MNs were retrogradely labeled with CtB conjugated to horseradish peroxidase, and revealed with diaminobenzidine (DAB). Although we have not collected any final data on this yet, the use of EM could also solve a potential confound present in our data by enhancing the resolution to better differentiate between GAD terminals that are in close contact of one another. EM will allow us to better quantify the amount of GAD65-IR terminals in contact with a single VGLUT1-IR terminal. Other methods are also available to solve the issue of resolution. For example, we have recently collected some images with a super-resolution technique using a Zeiss LSM 880 microscope with Airyscan. Images of MNs generated using this microscope have clearly distinguishable GAD65-IR terminals. Future experiments will take advantage of these techniques to better quantify the overall loss and change in size of the presynaptic inhibitory synapses opposing IA afferents.

In summary, the decrease in VGLUT1 boutons described here indicate a marginal reduction in the amount of IA afferent contacts onto MNs, whereas the analysis of presynaptic GAD65 boutons revealed a reduction in the amount of presynaptic inhibitory control that these IA contacts might receive following nerve crush. Respectively, these two phenomena are likely to contribute to 1) better preservation of stretch evoked EPSPs and 2) supranormal stretch reflex forces observed by Prather and colleagues (2011).

References

Abelew TA, Miller MD, Cope TC, Nichols TR (2000) Local loss of proprioception results in disruption of interjoint coordination during locomotion in the cat. J Neurophysiol 84:2709-2714.

Alvarez FJ, Titus-Mitchell HE, Bullinger KL, Kraszpulski M, Nardelli P, Cope TC (2011) Permanent central synaptic disconnection of proprioceptors after nerve injury and regeneration. I. Loss of VGLUT1/IA synapses on motoneurons. J Neurophysiol 106:2450-2470.

Bullinger KL, Nardelli P, Pinter MJ, Alvarez FJ, Cope TC (2011) Permanent central synaptic disconnection of proprioceptors after nerve injury and regeneration. II. Loss of functional connectivity with motoneurons. J Neurophysiol 106:2471-2485.

Castro-Lopes JM, Tavares I, Coimbra A (1993) GABA decreases in the spinal cord dorsal horn after peripheral neurectomy. Brain Res 620:287-291.

Cope TC, Bonasera SJ, Nichols TR (1994) Reinnervated muscles fail to produce stretch reflexes. Journal of Neurophysiology 71:817-820.

English AW, Chen Y, Carp JS, Wolpaw JR, Chen XY (2007) Recovery of electromyographic activity after transection and surgical repair of the rat sciatic nerve. J Neurophysiol 97:1127-1134.

Enriquez-Denton M, Manjarrez E, Rudomin P (2004) Persistence of PAD and presynaptic inhibition of muscle spindle afferents after peripheral nerve crush. Brain Res 1027:179-187.

Enriquez M, Jimenez I, Rudomin P (1996) Changes in PAD patterns of group I muscle afferents after a peripheral nerve crush. Exp Brain Res 107:405-420.

Gallego R, Kuno M, Nunez R, Snider WD (1980) Enhancement of synaptic function in cat motoneurones during peripheral sensory regeneration. J Physiol 306:205-218.

Haftel VK, Bichler EK, Wang QB, Prather JF, Pinter MJ, Cope TC (2005) Central suppression of regenerated proprioceptive afferents. J Neurosci 25:4733-4742.

Horch KW, Lisney SJ (1981) Changes in primary afferent depolarization of sensory neurones during peripheral nerve regeneration in the cat. J Physiol 313:287-299.

Hughes DI, Mackie M, Nagy GG, Riddell JS, Maxwell DJ, Szabo G, Erdelyi F, Veress G, Szucs P, Antal M, Todd AJ (2005) P boutons in lamina IX of the rodent spinal cord express high levels of glutamic acid decarboxylase-65 and originate from cells in deep medial dorsal horn. Proc Natl Acad Sci U S A 102:9038-9043.

Huyghues-Despointes CM, Cope TC, Nichols TR (2003) Intrinsic properties and reflex compensation in reinnervated triceps surae muscles of the cat: effect of activation level. J Neurophysiol 90:1537-1546.

Maas H, Prilutsky BI, Nichols TR, Gregor RJ (2007) The effects of self-reinnervation of cat medial and lateral gastrocnemius muscles on hindlimb kinematics in slope walking. Experimental brain research Experimentelle Hirnforschung Experimentation cerebrale 181:377-393.

Madison RD, Archibald SJ, Brushart TM (1996) Reinnervation accuracy of the rat femoral nerve by motor and sensory neurons. J Neurosci 16:5698-5703.

Mendell LM, Taylor JS, Johnson RD, Munson JB (1995) Rescue of motoneuron and muscle afferent function in cats by regeneration into skin. II. Ia-motoneuron synapse. J Neurophysiol 73:662-673.

Moore KA, Kohno T, Karchewski LA, Scholz J, Baba H, Woolf CJ (2002) Partial peripheral nerve injury promotes a selective loss of GABAergic inhibition in the superficial dorsal horn of the spinal cord. J Neurosci 22:6724-6731.

Navarro X (2009) Chapter 27: Neural plasticity after nerve injury and regeneration. Int Rev Neurobiol 87:483-505.

Nguyen QT, Sanes JR, Lichtman JW (2002) Pre-existing pathways promote precise projection patterns. Nat Neurosci 5:861-867.

Pierce JP, Mendell LM (1993) Quantitative ultrastructure of Ia boutons in the ventral horn: scaling and positional relationships. J Neurosci 13:4748-4763.

Pierce JP, Lewin GR (1994) An ultrastructural size principle. Neuroscience 58:441-446.

Portincasa A, Gozzo G, Parisi D, Annacontini L, Campanale A, Basso G, Maiorella A (2007) Microsurgical treatment of injury to peripheral nerves in upper and lower limbs: a critical review of the last 8 years. Microsurgery 27:455-462.

Prather JF, Nardelli P, Nakanishi ST, Ross KT, Nichols TR, Pinter MJ, Cope TC (2011) Recovery of proprioceptive feedback from nerve crush. J Physiol 589:4935-4947.

Rotterman TM, Nardelli P, Cope TC, Alvarez FJ (2014) Normal Distribution of VGLUT1 Synapses on Spinal Motoneuron Dendrites and Their Reorganization after Nerve Injury. The Journal of Neuroscience 34:3475-3492.

Sabatier MJ, To BN, Nicolini J, English AW (2011) Effect of slope and sciatic nerve injury on ankle muscle recruitment and hindlimb kinematics during walking in the rat. The Journal of Experimental Biology 214:1007-1016.

Scholz T, Krichevsky A, Sumarto A, Jaffurs D, Wirth GA, Paydar K, Evans GR (2009) Peripheral nerve injuries: an international survey of current treatments and future perspectives. J Reconstr Microsurg 25:339-344.

Taylor CA, Braza D, Rice JB, Dillingham T (2008) The incidence of peripheral nerve injury in extremity trauma. Am J Phys Med Rehabil 87:381-385.

Valero-Cabre A, Navarro X (2001) H reflex restitution and facilitation after different types of peripheral nerve injury and repair. Brain Res 919:302-312.